ELSEVIER

Journal of Arid Environments 66 (2006) 42–61

Journal of Arid Environments

www.elsevier.com/locate/jnlabr/yjare

Composition of aeolian dust in natural traps on isolated surfaces of the central Mojave Desert—Insights to mixing, sources, and nutrient inputs

R.L. Reynolds*, M. Reheis, J. Yount, P. Lamothe

US Geological Survey, MS 980, P.O. Box 25046, Denver, CO 80225, USA

Received 14 January 2005; received in revised form 17 May 2005; accepted 1 June 2005
Available online 20 December 2005

Abstract

The recognition and characterization of aeolian dust in soil contribute to a better understanding of landscape and ecosystem dynamics of drylands. Results of this study show that recently deposited dust, sampled in isolated, mostly high-ground settings, is chemically and mineralogically similar on varied geologic substrates over a large area (15 000 km^2) in the Mojave Desert. The silt-plus-clay fraction (fines) on these isolated surfaces is closely alike in magnetic-mineral composition, in contrast to greatly dissimilar magnetic compositions of rock surfaces of vastly different lithologies, on which the fines have accumulated. The fines, thus, are predominantly deposited dust. The amounts of potential nutrients in the sampled dust are much more uniform than might be provided by direct, local weathering of bedrock or by dust locally derived from nearby weathered products. The compositional similarity of the dust on these surfaces is interpreted to result from mixing of fines in the atmosphere as well as in fluvial, alluvial, and lacustrine depositional settings prior to dust emission.
Published by Elsevier Ltd.

Keywords: Aeolian dust; Magnetite; Magnetic properties; Plant nutrients; Mojave Desert

*Corresponding author. Tel.: +1 303 236 1303; fax: +1 303 236 5349.
E-mail addresses: rreynolds@usgs.gov (R.L. Reynolds), mreheis@usgs.gov (M. Reheis), yount@usgs.gov (J. Yount), plamothe@usgs.gov (P. Lamothe).

0140-1963/$ - see front matter Published by Elsevier Ltd.
doi:10.1016/j.jaridenv.2005.06.031

1. Introduction

Aeolian dust influences surficial and ecological processes in desert regions, where large amounts of dust are both sequestered and emitted over long periods of time (Goudie, 1978). In these settings, aeolian dust plays important roles in soil formation, soil hydrology, development of surfaces, distribution of biologic soil crusts, and nutrient status (e.g. Yaalon and Ganor, 1973; Wells et al., 1985, 1987; McFadden et al., 1986, 1987, 1998; Chadwick and Davis, 1990; McDonald et al., 1996; Belnap and Gillette, 1998; Shachak and Lovett, 1998; Reynolds et al., 2001a).

This paper reports primarily on the recognition and composition of aeolian dust on high surfaces, isolated from surrounding terrain, over an area of about 15 000 km^2 of the central Mojave Desert in the southwestern United States (Fig. 1). These isolated surfaces were sampled because the fine-grained sediment (fines) on them had no local alluvial source and thus must be primarily from dust. In the field, moreover, the fines at different sites were similar in color and magnetic susceptibility in contrast to variable characteristics of underlying bedrock. The principle goal of this study was to examine the compositional variation of dust in this setting over an area of diverse bedrock geology and geomorphology. Wells et al. (1982) previously interpreted fines in similar settings to be largely aeolian dust. The presence of aeolian dust in talus on steep dryland slopes (Whitney and Harrington, 1993; Blank et al., 1996) represents an analogous setting. Strong compositional similarity among distant sites would reflect the mixing of fines from disparate bedrock types. The mixing might occur in different ways, such as in surficial deposits that are dust sources and (or) in the atmosphere during dust transport. Compositional disparities might provide clues to dust sources and the physical processes, such as aerodynamic sorting of minerals, that control mineral-dust properties. Attention is also given to the potential nutrient loads of deposited dust because of their importance for biogeochemical dynamics.

Samples of fine-grained sediment on the isolated surfaces were collected from the surface down to only a few cm (typically 1–2 cm depth). These surfaces receive modern dust, but the time span represented by the entire sampled interval is not known and may vary among sites. It is likely that the sampled sediments represent dust deposited during at least the past few hundred years, as suggested by Reheis et al. (2002) for ‘old dust’ trapped in a comparable setting—vugs in volcanic rocks.

In this study we also compare dust collected on topographically isolated features with fine-grained sediment in surficial deposits at a few sites, most of them on alluvial fans, from approximately the same area to evaluate whether these different settings capture dust of similar or disparate properties. Significantly different properties might be attributable to proximity to local dust sources or to conditions causing spatial variability in dust deposition.

2. Setting

Sampled sites are in the central Mojave Desert, from Death Valley National Park southward to the Soda Lake area and the Cima volcanic field in the Mojave National Preserve (Fig. 1). This part of the Mojave is characterized by a variety of geologic surfaces that includes mountain ranges of diverse rock types, playas, ancient lake deposits, lava flows, sand-dune fields, alluvial fans, and riverbeds. In the northern part of the study area,

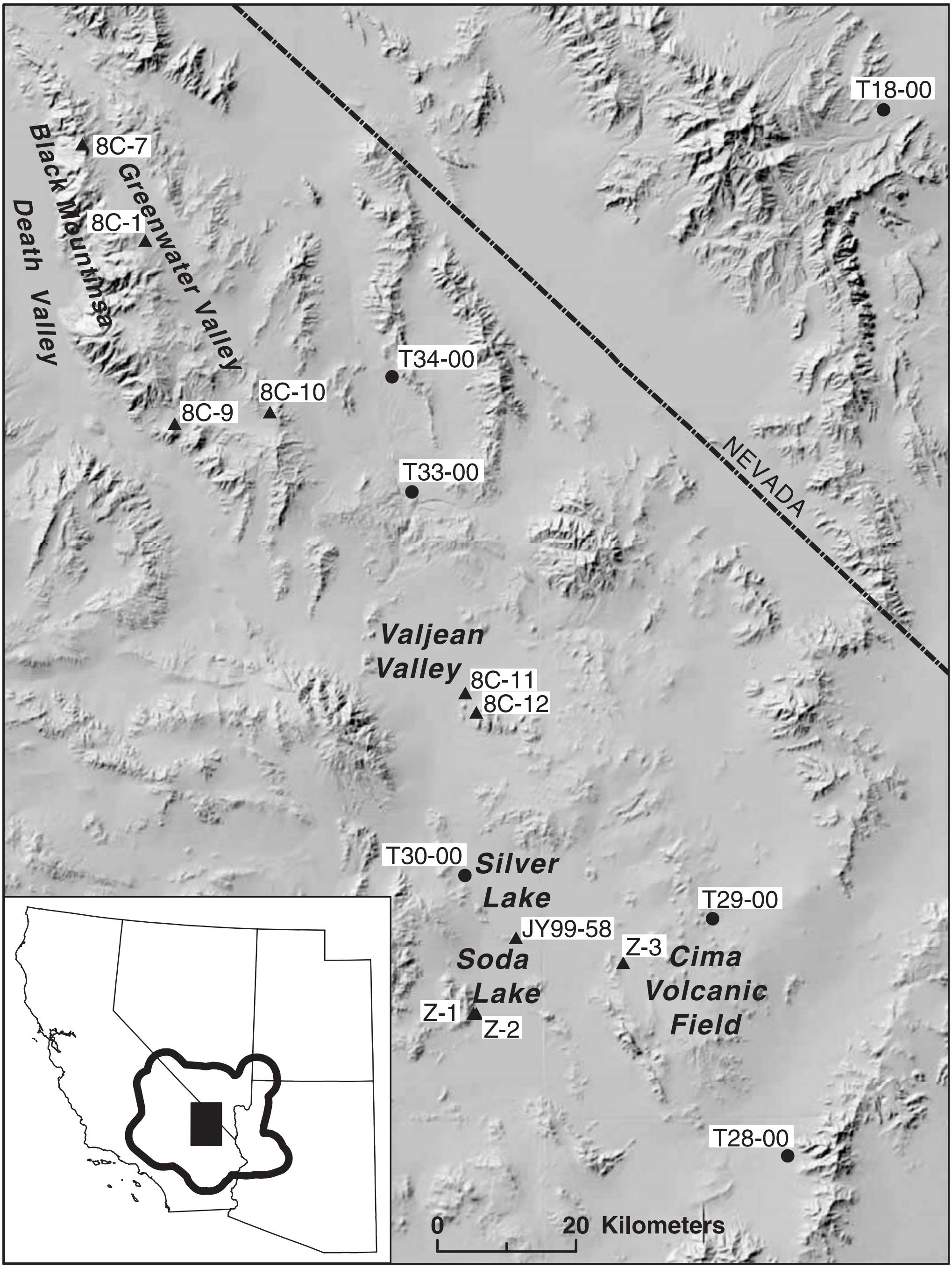

Fig. 1. Map showing locations of isolated sampling sites (triangles) and of soil samples near dust traps (trap sites; circles). Thick, solid line denotes the Mojave Desert within the index map of the southwestern United States.

Greenwater Valley and bounding ranges are dominantly underlain by middle Tertiary volcanic rocks, ranging mainly from andesitic to rhyolitic compositions (Drewes, 1963; Wright and Troxel, 1984; Workman et al., 2002). In the southern part, the Silurian Lake and Soda Lake areas, including Valjean Valley, are primarily underlain by granitic intrusions and a variety of metamorphic rocks, including quartzite and metalimestone. The Cima volcanic field, mainly composed of Pleistocene basalt flows and cones, lies at the southeastern edge of the study area.

3. Methods

3.1. Sampling

We sampled fine-grained material suspected to be primarily aeolian dust at 10 sites that included the tops of peaks and isolated high parts of ridges, as well as the surface of a mesa (site Z-3) (Fig. 1; Table 1). We collected the upper ~2 cm of fine-grained sediment found in pockets and crevices directly below summits. The sediment on the mesa was collected directly below rock clasts that formed a desert pavement; we also sampled a subjacent vesicular A soil layer. At most sites, fine-grained sediment was about 5–10 cm thick; the mantle of eolian sediment on the mesa was much thicker, perhaps 1–2 m, or more (see Wells et al., 1985). We did not observe evidence for physical or biologic disturbance at these sites. At each site, between 20 and 50 g of fine-grained material were obtained over an area of ~300–1000 cm^2, using a sharp-edged trowel. We also collected rock from outcrop, or from volcanic-rock clasts in the desert pavement at the site on the mesa (site Z-3). The setting at site Z-3, on a middle Pleistocene basalt flow in the Cima volcanic field, has been studied in detail with respect to dust-related development of desert pavement and soil (e.g. McFadden et al., 1986, 1998). Bedrock lithology and elevation range widely (Table 1). We compared results from these sites to new results on fines in the upper 0.5 cm of soil at six sites that spatially overlap the isolated sites (T-sites; Fig. 1; Table 1) and that are associated with dust traps, most of them in operation since 1984 (Reheis and Kihl, 1995). These sites were sampled in a manner closely similar to that for the sites on isolated surfaces. The trap sites, as we refer to them here, occur on a variety of surfaces of different geomorphic age, typically in valley floors and on alluvial fans. One of these sites (T29), however, occupied a high-elevation (about 1200 m a.s.l.) saddle between two cones in the Cima volcanic field. Site T29 is thus similar to the isolated sites with respect to its position above most of the surrounding landscape, but it likely is affected by local runoff, unlike the isolated sites.

3.2. Laboratory

The combination of chemical, mineralogic, and textural methods provides clear evidence for aeolian dust in desert surfaces (e.g. Marchand, 1970; Muhs, 1983; McFadden et al., 1987, 1998; Wells et al., 1987; Muhs et al., 1990; Reheis, 1990; Reheis et al., 1995; Naiman et al., 1999). In some settings, magnetic petrology, which characterizes magnetic minerals, may be a useful complement to these methods. Magnetic analyses (Thompson and Oldfield, 1986), together with reflected-light microscopy, were used to determine the types, amounts, and magnetic grain sizes of magnetic minerals. For petrographic analysis, magnetic minerals were prepared in polished grain mounts after isolation from the bulk sediment in a pumped-slurry magnetic separator (Reynolds et al., 2001b).

Table 1
Locations and settings of sampling sites (8C, Z, JY sites on isolated surfaces; T-group soil sites at dust traps)

Sample site	Latitude[a]	Longitude[a]	Elevation (m)	Setting	Setting—Location	Rock type[e]
8C-1	36 08.99	116 37.50	1622	Peak	Black Mountains	Rhyolite
8C-7	36 16.53	116 43.54	1859	Peak	Greenwater Valley	Andesitic breccia
8C-9	35 54.66	116 34.74	447	High point on ridge	Jubilee Pass	Schist
8C-10	35 55.54	116 25.59	1117	High point on ridge	Salisbury Pass	Altered volcanic breccia
8C-11	35 33.47	116 07.06	351	Peak	Valjean Valley	Quartzite
8C-12	35 31.95	116 06.03	603	Peak	Valjean Valley	Quartzite
Z-1	35 08.44	116 06.57	375	Peak	Soda Lake area (west)	Granite
Z-2	35 08.42	116 06.29	347	Peak	Soda Lake area (west)	Meta-limestone
Z-3	35 12.28	115 52.26	604	Mesa top	Desert pavement	Basalt
JY99-58	35 14.32	116 02.45	455	Peak	Soda Lake area (east)	Limestone
T18	36.31	115.44	1318	Alluvial fan[b]	North of Spring Mountains	Limestone, some quartzite
T28	34.95	115.61	921	Alluvial fan[c]	Southeast of Kelso Dunes	Mixed sedimentary and igneous
T29	35.26	115.73	1257	Basalt flow	Cima volcanic field	Basalt
T30	35.32	116.12	290	Alluvial fan[d]	West of Silver Lake	Meta-igneous
T33	35.31	116.14	366	Alluvial fan[c]	South side Tecopa basin	Mixed sedimentary and igneous
T34	35.97	116.23	525	Alluvial fan[b]	East side Tecopa basin	Limestone, some quartzite

[a]In degrees, decimal minutes (for 8C, Z, and JY sites); in degrees for T-group sites.
[b]Late Pleistocene fan.
[c]Middle (?) Pleistocene fan.
[d]Middle Holocene fan.
[e]Underlying bedrock lithology for isolated sites; bedrock lithology or dominant lithology of pavement clasts for soil sites at dust traps.

Magnetic measurements were made on dried sediment, sieved to isolate a silt-plus-clay fraction (fines), or rock fragments packed into 3.2-cm^3 plastic cubes and normalized for sample mass. A measure of the quantity of magnetite sufficiently large (magnetic grain size greater than about 30 nm) to carry remanence is isothermal remanent magnetization ($IRM_{0.3\,T}$), the magnetization acquired by a sample after exposure to a 0.3-T magnetic field. In this study, remanent magnetization was measured using a 90-Hz spinner magnetometer with a sensitivity of about $10^{-5}\,Am^{-1}$. Hard IRM (HIRM), a measure of high-coercivity ferric oxide minerals such as hematite, is calculated: $(IRM_{1.2\,T}–IRM_{0.3\,T})/2$. The ratio, $IRM_{0.3\,T}/IRM_{1.2\,T}$, called the S parameter, is a measure of the relative proportion of magnetite to all oxides, including hematite. High S values indicate large amounts of magnetite relative to hematite (a maximum value of 1), and decreasing values indicate increasing amounts of hematite. A measure for magnetic grain size is the ratio of anhysteretic remanent magnetization to $IRM_{0.3\,T}$ (ARM/IRM). Magnetic grain size, which may not indicate the physical size of a magnetite particle, reflects the magnetic domain structure of magnetic minerals thereby providing information about origins of these minerals. ARM/IRM values increase as the magnetic grain size of magnetite decreases, and it is particularly sensitive to single domain (SD) and small pseudo-single domain (PSD) magnetic grain sizes. ARM was imparted in a DC induction of 0.1 mT in the presence of a decaying alternating induction from 100 to 0 mT. Frequency-dependent magnetic susceptibility was determined to test for the presence of ultrafine (<30 nm) superparamagnetic magnetite or maghemite grains, which may form under pedogenic conditions (e.g. Dearing et al., 1996). No evidence for such pedogenic Fe oxides was found, and these results are not discussed further.

Particle size was determined on silt-plus-clay fractions as volume percentage using a laser-light scattering method capable of measuring particles greater than 0.5 μm, after removing organic matter using 30% hydrogen peroxide and carbonate using a 15% hydrochloric acid solution to eliminate any pedogenic carbonate in the soil. Such a treatment also removes any aeolian carbonate dust and detrital calcite, which might be locally derived from carbonate bedrock. Major, minor, and trace elements were determined on untreated fines using a combination of energy-dispersive X-ray fluorescence (XRF) and inductively coupled plasma (ICP-atomic emission spectroscopy and—mass spectroscopy; Lichte et al., 1987) analyses on pulverized samples.

Because samples from the topographically isolated sites and from the trap sites were initially analysed for separate studies, a different size portion was taken to represent the fines fraction. The <63 μm fraction represents fines from the topographically isolated sites, whereas the <50 μm fraction represents the fines from the trap sites, following analytical protocols (Reheis et al., 2002) for a group of long-term dust studies in the region.

4. Results

Magnetic properties of the fines on isolated surfaces are similar and, as a group, contrast greatly with the highly variable magnetic properties of the bedrock samples. Magnetite abundance in the fine fraction varies by about 2× (IRM, $1.99–3.90 \times 10^{-2}\,Am^2\,kg^{-1}$), hematite by 2.4× (HIRM, $1.28–3.12 \times 10^{-3}\,Am^2\,kg^{-1}$). In contrast, IRM and HIRM in rocks vary by about 3450× and 330×, respectively (Fig. 2a; Table 2). Concentration-independent parameters (ARM/IRM, magnetic grain size; and *S* parameter, relative amounts of magnetite and hematite) also cluster closely for the fines compared with those for bedrock samples (Fig. 2b). Among all sites, only one pair of fines and bedrock (site 8C-1 on rhyolite) exhibits closely similar magnetite content (Fig. 2a; Table 2). The fines and rock at this site, however, differ greatly in hematite content and in magnetic grain size, reflecting fundamentally different magnetic mineral suites (Fig. 2a; Table 2). Importantly, fines at nearby site 8C-7, on an exposure of andesite, have nearly identical magnetic properties as the fines at site 8C-1, but the two types of volcanic rock have significantly different amounts of magnetite and hematite (Fig. 2a, b; Table 2). The mineralogic similarities in the fines and their contrasts with the rocks can be explained only by aeolian dust at these sites, which do not receive alluvium or appreciable amounts of fine-grained colluvium.

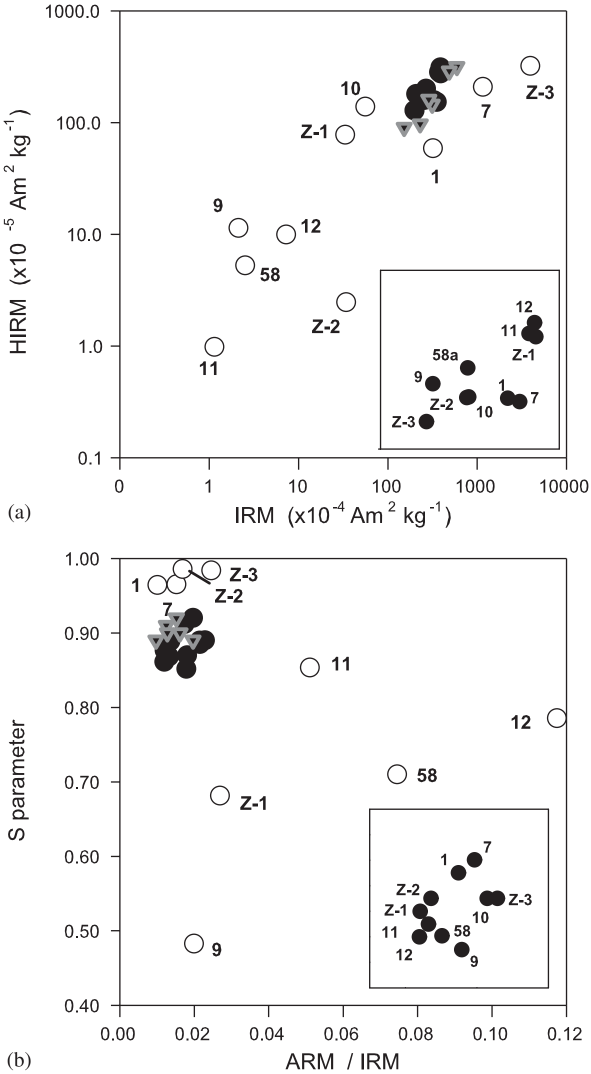

Fig. 2. (a) Plot of IRM (magnetite abundance) against HIRM (hematite abundance) for the fine fraction (solid symbols) and underlying bedrock (open symbols) at isolated sites, and for the fine fraction at trap sites (inverted triangles). (b) Plot of ARM/IRM (magnetic grain size of magnetite) against S parameter (magnetite relative to all magnetic minerals). Symbols as in (a) the ARM/IRM value for rock from site 8C-10 (0.205) is off scale. Insets show results from the fine-fraction samples at expanded scales to mark sites. Sites indicated without 8C- and JY99 prefixes. See text for magnetic property acronyms.

Petrographic examination qualitatively confirms the similarities of magnetic mineral suites in the fines as well as the great differences between these suites and the magnetic mineralogy of paired bedrock samples. At site 8C-1, for example, magnetic oxides in the rhyolite consist uniformly of magnetite phenocrysts partly replaced by hematite. In contrast, magnetic minerals in the fines are characterized by a wide variety of magnetic Fe–Ti oxides and associated Ti-rich phases, such as titanomagnetite in a variety of

Table 2
Summary of magnetic and silt-fraction results

Specimen	Type[a]	MS[b]	IRM[c]	HIRM[d]	S[e]	ARM[f]/IRM	C silt[g]	M silt[h]	F silt[i]
8C-1-1	s/c	2.35E−06	3.28E−02	1.58E−03	0.91	0.017	45	30	25
8C-1-2	Rock	2.46E−06	3.19E−02	5.88E−04	0.96	0.010			
8C-7-1	s/c	2.44E−06	3.53E−02	1.53E−03	0.92	0.020	43	28	29
8C-7-2	Rock	4.30E−06	1.16E−01	2.08E−03	0.97	0.015			
8C-9-1	s/c	1.72E−06	2.07E−02	1.80E−03	0.85	0.018	49	27	24
9C-9-2	Rock	3.57E−08	2.13E−04	1.14E−04	0.48	0.020			
8C-10-1	s/c	1.98E−06	2.58E−02	1.60E−03	0.89	0.021	36	29	35
8C-10-2	Rock	1.96E−07	5.59E−03	1.39E−03	0.67	0.205			
8C-11-1	s/c	2.97E−06	3.74E−02	2.83E−03	0.87	0.013	45	26	29
8C-11-2	Rock	1.87E−08	1.14E−04	9.82E−06	0.85	0.051			
8C-12-1	s/c	3.04E−06	3.87E−02	3.12E−03	0.86	0.012	54	26	20
8C-12-2	Rock	8.37E−09	7.27E−04	9.93E−05	0.79	0.117			
Z-1-1	s/c	3.13E−06	3.90E−02	2.75E−03	0.88	0.012	44	28	28
Z-1-2	Rock	1.64E−07	3.33E−03	7.78E−04	0.68	0.027			
Z-2-1	s/c	1.94E−06	2.55E−02	1.59E−03	0.89	0.014	31	31	38
Z-2-2	Rock	1.52E−07	3.42E−03	2.47E−05	0.99	0.017			
Z-3-2	s/c	1.36E−06	1.99E−02	1.28E−03	0.89	0.023	18	28	54
Z-3-3	Rock	9.59E−06	3.93E−01	3.21E−03	0.98	0.025			
JY99-58a	s/c	2.68E−06	2.57E−02	2.08E−03	0.86	0.015	24	17	59
JY99-58c	Rock	1.33E−08	2.53E−04	5.26E−05	0.71	0.075			

[a]s/c denotes silt plus clay sample.
[b]Magnetic susceptibility, in $m^3 kg^{-1}$.
[c]Isothermal remanent magnetization, in $Am^2 kg^{-1}$.
[d]Hard IRM, in $Am^2 kg^{-1}$.
[e]*S* parameter.
[f]Anhysteretic remanent magnetization.
[g]Coarse.
[h]Medium.
[i]Fine groups, as percentages, of the silt fraction (see text for particle-size ranges).

subdivided forms, chemically homogeneous magnetite, specular hematite, ilmenite, pseudobrookite, and numerous forms of ilmenorutile. Over the study area, no petrographic differences could be qualitatively discerned in the magnetic minerals in the fine fraction, regardless of associated bedrock type. By contrast, magnetic mineralogy of the bedrock was limited in mineral type at each site but varied greatly between sites. Some bedrock, such as quartzite, was devoid of strongly magnetic minerals. The presence of spherical magnetic particles (typically $<20\,\mu m$) in the fine fraction at many sites further distinguishes the magnetic mineral suites in the fine fraction from bedrock. These spherical particles were produced by coal combustion or other industrial activity (Locke and Bertine, 1986) and were transported long distances in the atmosphere to depositional sites.

The relatively small variation in magnetite abundance in the fines is reflected in their narrow range of iron abundance, compared to associated rocks (Fig. 3). With the exception of the fine-grained sample paired with basalt substrate (site Z-3), which contains abundant magnetite and iron, fines are enriched in Fe for a similar amount of magnetite in underlying bedrock. This relation is shown by a comparison of iron content and IRM for two sites (8C-1, and -7; Fig. 3) in the Greenwater Valley area (Fig. 1). Fines and volcanic

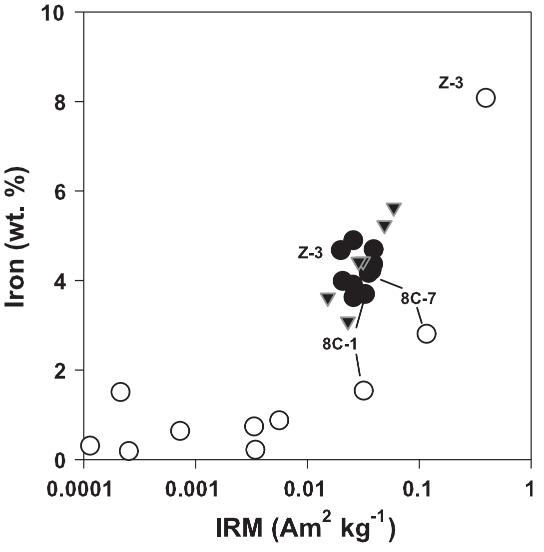

Fig. 3. Plot of iron against IRM (magnetite abundance). Symbols as in Fig. 2.

rock at 8C-1 have closely similar amounts of magnetite contents, but the fines have 2.4 × more iron. The fines at site 8C-7 have 3.3 × less magnetite but 1.5 × more iron than the underlying andesitic breccia.

Some elements reported here represent potential plant nutrients. Our chemical methods, however, show only concentrations of these elements and not the proportion available to plants. In the case of P especially, total concentration may be an unreliable indicator for plant-available P (Lajtha and Schlesinger, 1988). Most of these potential nutrients show tighter clusters of values compared with elemental contents of underlying bedrock (Fig. 4; Table 3). (Except for Mn vs. Cu, the plots pair elements that might be related by mineralogy or geologic association.) At most sites the fines are enriched in nearly all potential nutrients (potassium excepted) relative to the rocks (Fig. 4; Table 3). For each nutrient element, and for a few chemically stable elements, a measure of variation (range factor) is shown in Fig. 5 as the ratio of maximum value to minimum value. In most cases, there is little between-site variation (<2 ×) in the abundance of each element in the fines.

Phosphorus and Ca show the largest variations, but these variations are not related. The large range (6.8 ×) in P content is not linked to rock type, as indicated by a large difference at nearby sites on similar bedrock (e.g. sites 8C-11 and 12, on quartzite above Valjean Valley) and by disparate values at carbonate-rock settings (Z-2 vis-à-vis JY99-58). In contrast, the relatively large variations in Ca and Mg appear to be at least partly related to rock type. The highest Ca and Mg contents in fines (Ca = 7.4%, Mg = 3.5%; at site Z-2) reflect weathering of fine-grained carbonate rock (Ca = 30%, Mg = 12%). The small variation in titanium content (1.5 ×) in the fine-grained samples is similar to that of iron (Fig. 6a), as expected because of the close association of iron and titanium in many types of igneous rocks and detritus derived from them. In contrast, Zr varies by 2.7 × and Zr/Ti by 2.1 × (Figs. 5,6b).

Table 3
Chemical results for samples of fines (s/c) and rocks from isolated sites

Specimen	Type[a]	Al (%)	Ca (%)	K (%)	Na (%)	Mg (%)	Mn (ppm)	P (%)	Cu (ppm)	Zn (ppm)	Ti (%)	Fe (%)	Zr (ppm)
8C-1-1	s/c	7.50	2.60	2.70	1.60	1.60	730	0.22	27	99	0.49	3.70	414
8C-1-2	Rock	7.60	1.90	3.40	2.30	0.50	390	0.06	7	40	0.20	1.54	132
8C-7-1	s/c	8.80	2.20	3.20	2.00	1.80	870	0.08	36	180	0.53	4.17	394
8C-7-2	Rock	7.90	0.94	7.80	1.30	1.00	1100	0.1	8	180	0.39	2.81	115
8C-9-1	s/c	7.50	5.20	2.90	1.40	1.80	960	0.12	24	120	0.54	3.99	554
9C-9-2	Rock	6.00	0.46	3.10	1.80	0.28	260	0.03	7	32	0.15	1.51	114
8C-10-1	s/c	7.60	4.50	2.80	1.60	1.70	900	0.18	25	100	0.49	3.63	405
8C-10-2	Rock	6.20	5.00	7.30	0.72	0.06	240	0.03	5	14	0.09	0.88	101
8C-11-1	s/c	7.60	2.90	2.50	1.80	1.80	950	0.27	25	110	0.64	4.23	825
8C-11-2	Rock	0.32	0.02	0.12	0.01	0.02	33	0.01	6	2	0.02	0.31	53
8C-12-1	s/c	7.70	2.90	2.50	1.80	1.80	980	0.17	22	110	0.68	4.37	865
8C-12-2	Rock	2.00	0.07	1.00	0.02	0.15	50	0.02	4	15	0.07	0.64	70
Z-1-1	s/c	7.70	2.60	2.30	1.80	1.60	970	0.21	27	100	0.71	4.70	1072
Z-1-2	Rock	5.10	0.37	3.00	2.50	0.04	290	0.009	9	51	0.06	0.74	151
Z-2-1	s/c	6.80	7.40	2.10	1.60	3.50	1000	0.24	31	100	0.53	3.91	628
Z-2-2	Rock	0.44	30.00	0.31	0.03	12.00	1400	0.02	0	5	0.01	0.22	19
Z-3-2	s/c	7.80	5.00	2.90	1.80	2.00	840	0.19	40	120	0.60	4.68	402
Z-3-3	Rock	8.80	6.60	1.50	3.00	4.90	1600	0.32	37	91	1.53	8.08	275
JY99-58	s/c	7.92	2.95	2.63	1.94	1.24	918	0.55	30	93	0.59	4.90	648
JY99-58	Rock	0.23	34.50	0.01	0.01	0.60	2110	0.01	12	29	0.02	0.19	35

[a]s/c denotes silt plus clay sample.

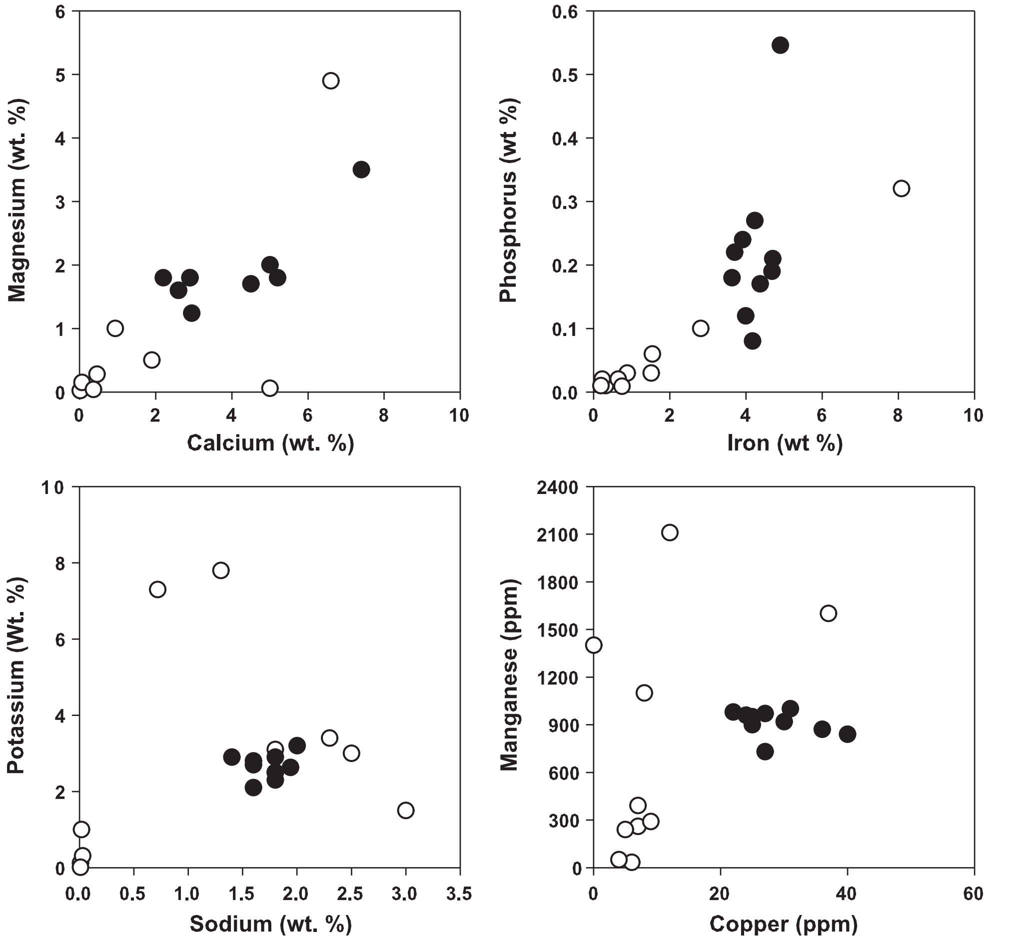

Fig. 4. Bivariate plots of elemental abundance for the fine fraction (solid symbols) and underlying bedrock (open symbols) at isolated sites. Calcium data for carbonate bedrock at sites Z-2 and JY99-58 are off scale (see Table 3).

The magnetic-mineral and chemical compositions of the fines from the isolated sites mostly overlap those of fines from the trap sites. Magnetic properties of the two groups have closely similar ranges (Fig. 2). For elements analysed in common (Table 4), there are no significant differences in the group averages at $p<0.05$, except for Ti and Zr, both of which are higher in the trap-site soil samples.

5. Discussion

5.1. Compositional similarities—evidence for mixing of fines

The overall compositional similarities of the dust on the isolated, widely separated, and geologically diverse surfaces are interpreted to reflect mixing of aeolian sediment from multiple sources. Such mixing likely has taken place in different environments—in the

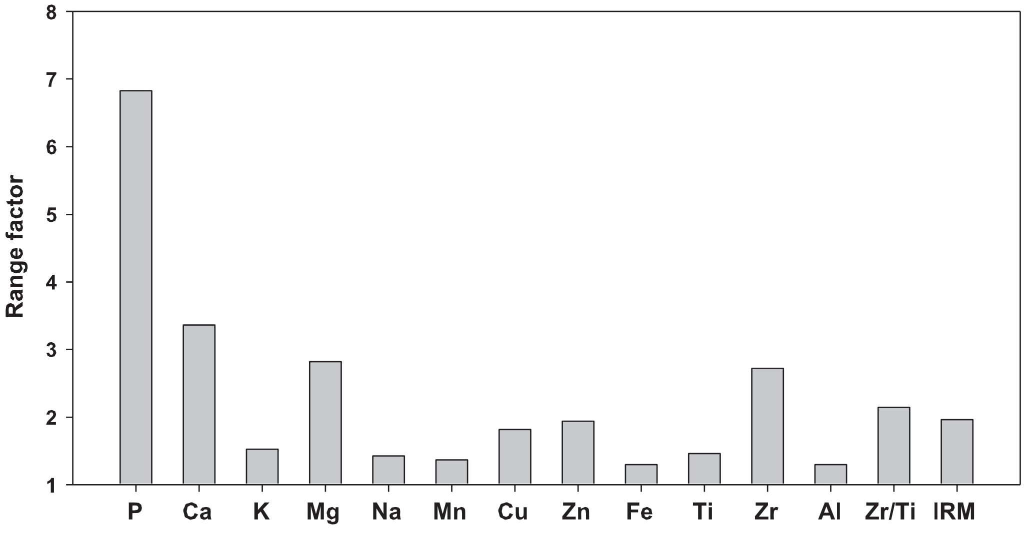

Fig. 5. Amount of variation for selected elements, Zr/Ti, and IRM in the fine-grained fraction from isolated sites. The range factor is the ratio of maximum value to minimum value for each element at all sites.

atmosphere as well as in fluvial, alluvial, and lacustrine depositional settings prior to dust entrainment. Observations of contemporary dust events and storms in the Mojave Desert indicate that many windstorms, even those of modest strength and duration, simultaneously generate dust plumes from many sources and geomorphic settings and that areas of fallout from different plumes commonly overlap (Chavez et al., 2002; Reynolds et al., 2003). Such sources today include varieties of both natural settings and disturbed settings in areas of recreation, infrastructure development, military activity, and agriculture, as examples. Drainage systems, including the channels of alluvial fans, small washes, and major river systems (such as the Amargosa and Mojave Rivers) are sites of surficial mixing of fine-grained sediment from numerous bedrock lithic types. Contemporary observations and compositions of modern dust (Reheis and Kihl, 1995) indicate that typically dry floodplains of large drainages, in particular, are prolific sources of dust. Playas, which accumulate fine-grained sediment from many sources, may also be sites of dust emission (Gill, 1996; Reheis et al., 2002), the degree to which depends on many factors, perhaps most importantly their hydrology and as well as type and degree of surface disturbance.

Strong similarities in chemical and mineralogical composition among modern dust samples from different geographic areas with dissimilar dust sources in the southwestern US (Reheis and Kihl, 1995; Reheis et al., 2002) show that dusts undergo mixing in the atmosphere prior to deposition. Such mixing, modified perhaps by aerodynamic sorting within plumes, is also demonstrated by the downwind dilution of salt-rich, chemically distinct dust (enriched in As, Ba, Li, and Sb) derived from the dry bed of Owens Lake (Reheis, 1997; Reheis et al., 2002). For example, As and Sb in dust samples appear to decrease gradually with distance from Owens Valley, whereas Ba and Li are elevated only in dust samples from within Owens Valley.

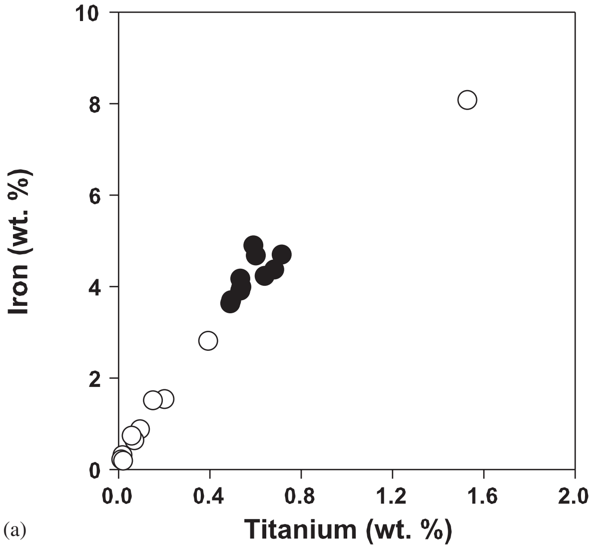

(a)

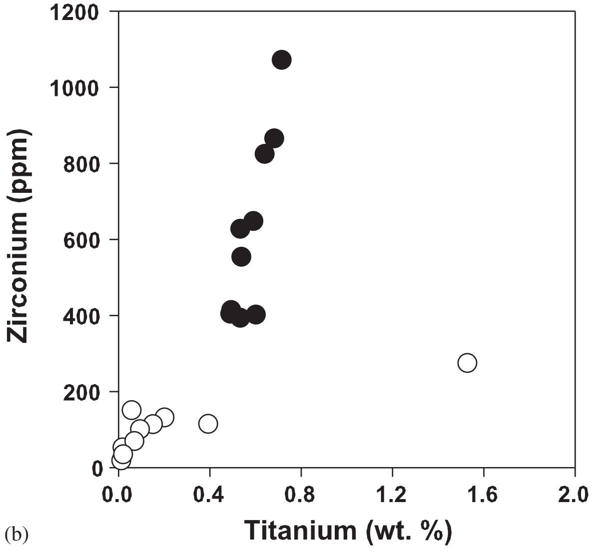

(b)

Fig. 6. Bivariate plots of elemental abundance for the fine fraction (solid symbols) and underlying bedrock (open symbols) at isolated sites: (a) plot of iron against titanium and (b) plot of zirconium against titanium.

5.2. Compositional variability—evaluation of aerodynamic sorting and pedogenesis

We examined chemical, magnetic, and textural data, along with geographic setting, for evidence that relatively small compositional variations in surface fines could be attributed to physical sorting and (or) chemical alteration. In one approach, we assessed Ti, Zr, Fe, and magnetic properties, because variations among them in sediments commonly elucidate changes in source areas and (or) influence by sorting processes (Rosenbaum et al., 1996; Reynolds et al., 2001a). As an example, differences in Ti and Zr in late Pleistocene loess

Table 4
Chemical results for samples from isolated-surface (8C, Z, JY specimens) and trap (soil at trap; T-group) sites for elements analysed in common

Specimen	Ca (%)	Fe (%)	Ti (%)	Zr (ppm)	Zr/Ti	Fe/Ti	Ba (ppm)	Ce (ppm)	Cr (ppm)	La (ppm)	Li (ppm)	Ni (ppm)	Pb (ppm)	Th (ppm)
8C-1-1	2.60	3.70	0.49	414	0.08	7.5	690	99	56	50	50	25	30	18
8C-7-1	2.20	4.17	0.53	394	0.07	7.83	1200	110	66	65	80	31	33	20
8C-9-1	5.20	3.99	0.54	554	0.10	7.42	770	140	52	74	61	25	53	24
8C-10-1	4.50	3.63	0.49	405	0.08	7.42	680	120	52	62	58	27	32	22
8C-11-1	2.90	4.23	0.64	825	0.13	6.62	770	160	59	82	45	26	33	31
8C-12-1	2.90	4.37	0.68	865	0.13	6.41	720	160	69	79	42	30	33	30
Z-1-1	2.60	4.70	0.71	1072	0.15	6.58	690	170	72	88	44	28	35	32
Z-2-1	7.40	3.91	0.53	628	0.12	7.34	590	130	62	64	58	29	30	22
Z-3-2	5.00	4.68	0.60	402	0.07	7.79	530	110	63	58	66	34	27	21
JY99-58	2.95	4.90	0.59	648	0.11	8.31	na	na	na	na	na	na	na	na
T18-00	8.93	3.09	0.54	738	0.14	5.69	513	98	54	50	29	21	35	17
T28-00	4.01	4.43	0.82	894	0.11	5.41	703	143	60	72	38	25	34	25
T29-00	2.62	5.63	1.18	1610	0.14	4.77	638	178	90	92	40	33	28	34
T30-00	3.34	5.24	0.88	1100	0.12	5.95	661	157	63	81	43	25	39	30
T33-00	6.51	3.62	0.51	491	0.10	7.17	522	123	50	60	135	25	41	22
T34-00	5.24	4.42	0.81	987	0.12	5.48	619	187	66	94	84	26	34	32
p^{a}	0.217	0.703	0.017	0.038	0.201	0.001	0.143	0.363	0.652	0.475	0.720	0.181	0.741	0.482

na, not analysed.
[a]Probability associated with Student's *t*-test in comparisons between samples from the isolated-surface and trap sites.

have been attributed to downwind sorting of relatively fine-grained Ti-bearing minerals (presumably forms of TiO_2) from coarser Zr-bearing minerals (Mason and Jacobs, 1998; Muhs and Bettis, 2000).

Comparisons among chemical, magnetic, and textural data do not show strong evidence for sorting. For these comparisons, we analysed the silt-fraction data as three groups—coarse, 31.2–63 μm; medium, 15.6–31.2 μm; and fine, 3.9–15.6 μm. Using regression analysis, the different particle-size ranges within the silt groups do not correlate with Ti, Zr, or Zr/Ti, or with magnetite amounts (Table 2). Moreover, the silt groups do not show correspondence to elevations of the sites. Although aerodynamic sorting takes place in atmospherically entrained dust, sorting does not emerge as a dominant influence on differences in compositional properties of our samples.

Particle-size distributions within the total silt fraction were also examined for evidence of source-area or sorting influence. The silt fraction in most samples is dominantly coarse and (or) medium silt (Fig. 7). As an exception, two samples from site Z3 (the surface fines and underlying vesicular A horizon on the basaltic mesa) are dominated by fine silt that may reflect high dust content from Soda Lake (see McFadden et al., 1986). Two samples from the Hanks Mountain site (JY99-58; in carbonate rock) are enriched in both very fine silt and coarse silt. This site is only 4 km from the northwestern margin of Soda Lake and thus is expected to capture playa dust. Coarse silt at this site reflects the presence of local aeolian sand at this near-summit site that was derived from washes below (see Lancaster, 1997). The textural results suggest that most sites are not distributed at sufficient distances from themselves and from sources to record systematic, regional variations in particle-size distribution of dust related to atmospheric sorting processes. The results also illustrate that large variation in particle sizes are not expressed as compositional differences of the fines.

Comparison of chemical and magnetic properties of fines on isolated surfaces to those of trap-site fines does not reveal large systematic differences that indicate a strong influence by atmospheric sorting. The significantly higher amounts of both Ti and Zr in the trap-site

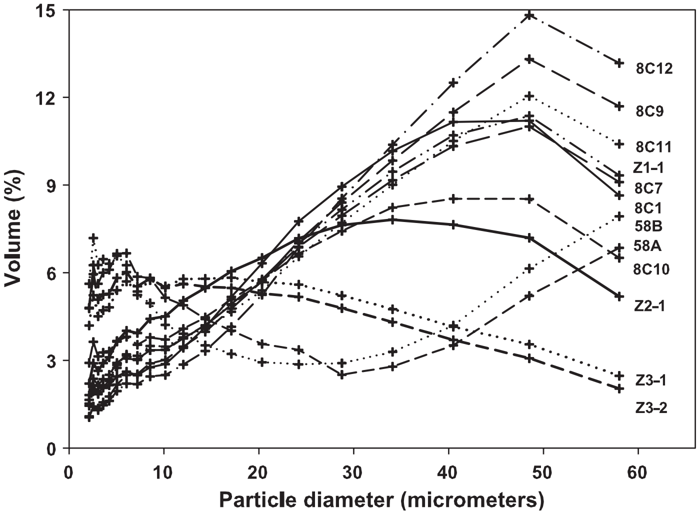

Fig. 7. Particle-size distribution for the normalized silt fraction. Lines connect data points (+) that represent the mid-points of 20 measured particle-size intervals.

samples imply higher amounts of certain heavy minerals (e.g. rutile and zircon) in these sites, weakly suggesting that aerodynamic sorting has affected the distribution of some heavy minerals. Testing this possibility would require study of a larger area.

Another process that may produce differences in the chemical composition of shallow samples is pedogenic modification involving leaching of relatively soluble components. For example, depletions of NaO and K_2O from shallow dust-dominated soils (the Av horizon) on the piedmont of the Soda Mountains within the study area are attributed to leaching, on the basis of comparing measured soil-horizon compositions with modeled compositions from mixed proportions of parent material and inferred dust constituents (McFadden et al., 1998). Smaller depletions of CaO and MgO in near-surface soil appear to be expressed in accumulation of pedogenic carbonate in lower horizons (McFadden et al., 1998). Our shallow sampling was not designed to evaluate the degree of leaching of soluble components. The small variations in abundances of Na and K (Figs. 4 and 5) suggest that any such leaching at our sites was not highly variable. Larger variability in amounts of Ca and Mg is attributed to the effects of weathering of carbonate bedrock, rather than to leaching.

5.3. *Dust and potential plant nutrients*

To examine potential nutrients in the dust and relations to sources, we determined a nutrient index for each dust sample and compared these indices to magnetic properties. Here, the nutrient index is the sum of selected elements that have been normalized to the highest value of a given element in the dataset. Magnetite abundance shows no relation to the nutrient index composed of K, Mg, P, Cu, Mn, Zn, and Fe, elements that are dominantly derived from non-carbonate rock (Fig. 8a). This observation contrasts with results from surficial deposits on the central Colorado Plateau that demonstrated a close correlation between far-traveled aeolian magnetite and potential nutrients in surficial deposits on nutrient-poor bedrock units, which lack magnetite over large areas of the region (Reynolds et al., 2001a, 2005). The plot of IRM against an index for Ca and Na, elements that may be derived in large amounts from the surfaces of currently evaporative playas, shows that relatively high values of this index correspond with relatively low abundance of magnetite (Fig. 8b; $r^2 = 0.71$; $p < 0.05$). This negative correlation suggests that relatively low magnetite content in this region identifies relatively high dust contributions from playas, which are low in magnetite content because of (a) dilution by chemically precipitated minerals and (or) (b) low-energy environments of sedimentation.

The relatively high variation in P abundance at our sites (Figs. 4 and 5) is noteworthy because P can limit productivity in drylands (Guevara et al., 2000; Snyman, 2002) and because P concentrations appear to vary widely across arid and semi-arid ecosystems (Lajtha and Schlesinger, 1988; J.C. Neff, pers. comm., 2004). In eight of ten sites, fines contained much higher P amounts than found in associated bedrock at the sites (Table 3). Whatever the causes of the observed variations in P at our sites, the results indicate that aeolian dust provides an important avenue for P inputs to the Mojave ecosystem. More work is required to examine possible links between dust and plant-available P in the study area.

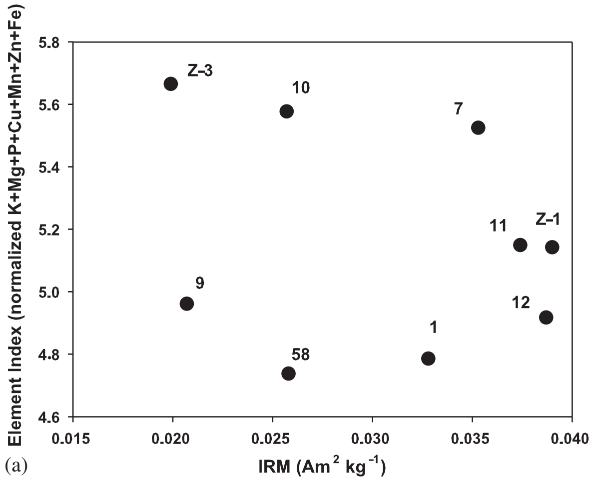

(a)

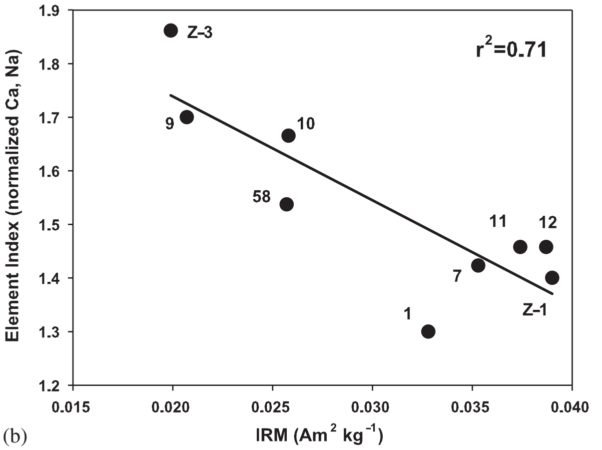

(b)

Fig. 8. Plots of nutrient index vs. IRM. (a) The element index is the sum of normalized abundances of K, Mg, P, Cu, Mn, Zn, and Fe. (b) The element index is the sum of normalized abundances of Ca and Na.

6. Conclusions

Dust deposited on widely separated, isolated settings in the Mojave Desert are similar in mineralogic and chemical composition, regardless of underlying bedrock composition. These overall compositional similarities reflect mixing of fines from multiple sources. Such mixing likely has taken place in the atmosphere as well as in fluvial, alluvial, and lacustrine settings. Compositional variation in dust from these isolated sites is similar to that in fines from the mainly intermontane soil settings in the study area.

Additions of well-mixed dust to soils formed on bedrock and derived colluvium and alluvium of widely different lithologic and chemical compositions serve to homogenize the near-surface sediment (beneath desert pavement, if present) to a much more uniform state (e.g. McFadden et al., 1986; McDonald, 1994; Reheis et al., 1995) that closely resembles desert dust. This surficial sediment is the horizon in which most seed germination occurs and in which resides much of the available water-holding capacity of aridic soils (e.g. McDonald et al., 1996; McFadden et al., 1998). Thus, the potential nutrient load of shallow soils across the central Mojave Desert may be very broadly approximated by the composition of aeolian dust.

In nearly all comparisons, fines (predominantly aeolian dust) contain elevated amounts of magnetic minerals and elemental contents relative to associated rocks. These differences may partly result from sampling design. We sampled surfaces of a broad range of bedrock types rather than surfaces proportionally representative of the substrates in the study area. Relatively high content of magnetite and hematite in the dust on isolated surfaces is notable, because these minerals have high specific gravity and are thereby especially subject to aerodynamic sorting during aeolian transport. Sorting has not noticeably influenced the iron oxide composition of the dust at our sites on isolated surfaces, in view of the lack of related patterns among contents of high-density magnetic minerals, chemical proxies for heavy minerals (Ti, Zr), proportions of fine-, medium-, and coarse-silt fractions, geographic distribution, and elevation. A similar study over a larger area, investigating dust collected on Jurassic sedimentary rocks in a transect from the eastern Mojave Desert to the Colorado Plateau, revealed systematic decreases in amounts of magnetite and titanium eastward (Goldstein et al., 2002), as expected for removal of these components by aerodynamic sorting away from their predominant source areas.

An initial objective of this study was to evaluate the feasibility of magnetic methods to detect aeolian dust in Quaternary surfaces in the complicated geologic and magnetic setting of the central Mojave Desert. The magnetic technique consists of comparing the types and amounts of magnetic minerals in surficial deposits with magnetic minerals in nearby rock or coarse-grained sediment, the weathering of which might alternatively produce fine-grained sediment. In this study, the method provided quantitative measure of a mineral suite that documents aeolian dust, showing that these minerals in the fine fraction of surficial deposits were not derived from bedrock substrates. Our results thus indicate that magnetic methods can be used to identify aeolian dust in geologically complex arid-land settings over large areas.

Acknowledgments

We express deep gratitude to Harland Goldstein for invaluable assistance in sample and data management, to Nilah Mazza, Jiang Xiao, and Eric Fisher for physical property measurements, to Fred Luiszer for XRF analyses, and to Jeremy Workman and Ren Thompson for discussions about the geology of the Death Valley region. The manuscript benefited from reviews by Jayne Belnap, Harland Goldstein, Jason Neff, and two anonymous referees. This work was supported by the Earth Surface Dynamics Program of the US Geological Survey.

References

Belnap, J., Gillette, D.A., 1998. Vulnerability of desert biological soil crusts to wind erosion: the influences of crust development, soil texture, and disturbance. Journal of Arid Environments 39, 133–142.

Blank, R.R., Young, J.A., Lugaski, T., 1996. Pedogenesis on talus slopes, the Buckskin Range, Nevada, USA. Geoderma 71, 121–142.

Chadwick, O.A., Davis, J.O., 1990. Soil-forming intervals caused by eolian sediment pulses in the Lahontan basin, northwestern Nevada. Geology 18, 243–246.

Chavez, P.S., Jr., MacKinnon, D.J., Reynolds, R.L., Velasco, M., 2002. Monitoring dust storms and mapping landscape vulnerability to wind erosion using satellite and ground-based digital images. Arid Lands Newsletter 51, web publication: http://ag.arizona.edu/OALS/ALN/aln51/chavez.html.

Dearing, J.A., Hay, K.L., Baban, M.J., Huddleston, A.S., Wellington, E.M., Loveland, P.J., 1996. Magnetic susceptibility of soil: an evaluation of conflicting theories using a national data set. Geophysical Journal International 127, 728–734.

Drewes, H., 1963. Geology of the Funeral Peak Quadrangle, California, on the East Flank of Death Valley. US Geological Survey Professional Paper 413, 78p.

Gill, T.E., 1996. Eolian sediments generated by anthropogenic disturbance of playas: human impacts on the geomorphic system and geomorphic impacts on the human system. Geomorphology 17, 207–228.

Goldstein, H., Reheis, M., Reynolds, R.L., Yount, J., Simmons, K., Lamothe, P., Luiszer, F., 2002. Aeolian dust on isolated surfaces from the Mojave Desert to the Colorado Plateau, USA. In: Lee, J.A., Zoback, T.M. (Eds.), Proceedings of ICAR5/GCTE-SEN Joint Conference, Lubbock, Texas. International Center for Arid and Semiarid Lands Studies, Texas Tech University Publication 02-2, pp. 314–316.

Goudie, A.S., 1978. Dust storms and their geomorphological implications. Journal of Arid Environments 1, 291–310.

Guevara, J.C., Stasi, C.R., Estevez, O.R., Le Houerou, H.N., 2000. N and P fertilization on rangeland production in Midwest Argentina. Journal of Range Management 53, 410–414.

Lajtha, K., Schlesinger, W.H., 1988. The biogeochemistry of phosphorus cycling and phosphorus availability along a desert soil chronosequence. Ecology 69, 24–39.

Lancaster, N., 1997. Response of eolian geomorphic systems to minor climate change: examples from the southern California deserts. Geomorphology 19, 333–347.

Lichte, F.E., Golightly, D.W., Lamothe, P.J., 1987. Inductively coupled plasma-atomic emission spectrometry. In: Baedecker, P.A. (Ed.), Methods for Geochemical Analysis. US Geological Survey Bulletin 1770, pp. B1–B10.

Locke, G., Bertine, K.K., 1986. Magnetite in sediments as an indicator of coal combustion. Applied Geochemistry 1, 345–356.

Marchand, D.E., 1970. Soil contamination in the White Mountains, eastern California. Geological Society of America Bulletin 81, 2497–2506.

Mason, J.A., Jacobs, P.M., 1998. Chemical and particle-size evidence for addition of fine dust to soils of the midwestern United States. Geology 26, 1135–1138.

McDonald, E.V., 1994. The relative influence of climatic change, desert dust, and lithologic control on soil-geomorphic processes and hydrology of calcic soils formed on Quaternary alluvial fan deposits in the Mojave Desert, California, Albuquerque, NM. Ph.D. Dissertation, University of New Mexico, 383pp.

McDonald, E.V., Pierson, F.B., Flerchinger, G.N., McFadden, L.D., 1996. Application of a process-based soil–water balance model to evaluate the influence of Late Quaternary climate change on soil–water movement in calcic soils. Geoderma 74, 167–192.

McFadden, L.D., Wells, S.G., Dohrenwend, J.C., 1986. Influences of Quaternary climatic changes on processes of soil development on desert loess deposits of the Cima volcanic field, California. Catena 13, 361–389.

McFadden, L.D., Wells, S.G., Jercinovich, M.J., 1987. Influences of eolian and pedogenic processes on the origin and evolution of desert pavements. Geology 15, 504–508.

McFadden, L.D., McDonald, E.V., Wells, S.G., Anderson, K., Quade, J., Forman, S.L., 1998. The vesicular layer and carbonate collars of desert soils and pavements: formation, age, and relation to climate change. Geomorphology 24, 101–145.

Muhs, D.R., 1983. Airborne dust fall on the California Channel islands, USA. Journal of Arid Environments 6, 223–238.

Muhs, D.R., Bettis, E.A., 2000. Geochemical variations in Peoria Loess of western Iowa indicate paleowinds of midcontinental North America during last glaciation. Quaternary Research 53, 49–61.

Muhs, D.R., Bush, C.A., Stewart, K.C., Rowland, T.R., Crittenden, R.D., 1990. Geochemical evidence of Saharan dust parent material for soils developed on Quaternary limestones of Caribbean and western Atlantic islands. Quaternary Research 33, 157–177.

Naiman, Z., Quade, J., Patchett, P.J., 1999. Strontium, carbon, and oxygen isotope evidence for eolian recycling of pedogenic carbonate. Geochimica Cosmochimica Acta 64, 3099–3109.

Reheis, M.C., 1990. Influence of climate and eolian dust on the major-element chemistry and clay minerals of soils in the northern Bighorn basin, USA. Catena 17, 219–248.

Reheis, M.C., 1997. Dust deposition downwind of Owens (dry) lake, 1991–1994: preliminary findings. Journal of Geophysical Research 102, 25999–26008.

Reheis, M.C., Kihl, R., 1995. Dust deposition in southern Nevada and California, 1984–1989: relations to climate, source area, and source lithology. Journal of Geophysical Research 100, 8893–8918.

Reheis, M.C., Goodmacher, J.C., Harden, J.W., McFadden, L.D., Rockwell, T.K., Shroba, R.R., Sowers, J.M., Taylor, E.M., 1995. Quaternary soils and dust deposition in southern Nevada and California. Geological Society of America Bulletin 107, 1003–1022.

Reheis, M.C., Budahn, J.R., Lamothe, P.J., 2002. Geochemical evidence for diversity of dust sources in the southwestern United States. Geochimica et Cosmochimica Acta 66, 1569–1587.

Reynolds, R.L., Belnap, J., Reheis, M., Lamothe, P., Luiszer, F., 2001a. Eolian dust in Colorado Plateau soils: nutrient inputs and recent change in source. Proceedings of the National Academy of Sciences 98, 7123–7127.

Reynolds, R.L., Sweetkind, D.S., Axford, Y., 2001b. An inexpensive magnetic mineral separator for fine-grained sediment. US Geological Survey Open-file Report 01-281.

Reynolds, R.L., Reheis, M., Chavez, P., Hinkley, T., Tigges, R., Clow, G., MacKinnon, D., Lamothe, P., Lancaster, N., Miller, M., Yount, J., Velasco, M., Sides, S., Soltesz, D., Meeker, G., Fulton, R., Belnap, J., 2003. Dust emission and deposition in the southwestern US—integrated field, remote sensing, and modeling studies to evaluate response to climatic variability and land use. In: Al Sharhan, A.R., Wood, W.W., Goudie, A.S., Fowler, A., Abdellatif, E. (Eds.), Desertification in the Third Millennium. Swets & Zeitlinger, Lisse, The Netherlands, pp. 271–282.

Reynolds R.L., Neff, J.C., Reheis, M.C., Lamothe, P., 2005. Atmospheric dust in modern soil on aeolian sandstone, central Colorado Plateau Utah: variation with landscape position and contribution to potential plant nutrients. Geoderma, in press.

Rosenbaum, J.G., Reynolds, R.L., Adam, D.P., Drexler, J., Sarna-Wojcicki, A.M., Whitney, G.C., 1996. Record of middle Pleistocene climate change from Buck Lake, Cascade Range, southern Oregon—evidence from sediment magnetism, trace-element geochemistry, and pollen. Geological Society of America Bulletin 108, 1328–1341.

Shachak, M., Lovett, G.M., 1998. Atmospheric deposition to a desert ecosystem and its implications for management. Ecological Applications 8, 455–463.

Snyman, H.A., 2002. Short-term response of rangeland botanical composition and productivity to fertilization (N and P) in a semi-arid climate of South Africa. Journal of Arid Environments 50, 167–183.

Thompson, R., Oldfield, F., 1986. Environmental Magnetism. Allen Unwin, London.

Wells, S.G., Ford, R.L., Grimm, J.P., Martinez, G.F., Pickle, J.D., Sares, S.W., Weadock, G.L., 1982. Development of debris mantled hillslopes: an example of feedback mechanisms in desert hillslope processes. In: Leopold, L.B. (Ed.), 1982 Conference Field Trip Guidebook. American Geomorphological Field Group, Pinedale Wyoming, p. 141.

Wells, S.G., Dohrenwend, J.C., McFadden, L.D., Turrin, B.D., Mahrer, K.D., 1985. Late Cenozoic landscape evolution on lava flow surfaces of the Cima volcanic field, Mojave Desert, California. Geological Society of America Bulletin 96, 1518–1529.

Wells, S.G., McFadden, L.D., Dohrenwend, J.C., 1987. Influence of late Quaternary climatic changes on geomorphic and pedogenic processes on a desert piedmont, eastern Mojave Desert, California. Quaternary Research 27, 130–146.

Whitney, J.W., Harrington, C.D., 1993. Relict colluvial boulder deposits as paleoclimatic indicators in the Yucca Mountain region, southern Nevada. Geological Society of America Bulletin 105, 1008–1018.

Workman, J.B., Menges, C.M., Page, W.R., Taylor, E.M., Ekren, E.B., Rowley, P.D., Dixon, G.L., Thompson, R.A., Wright, L.A., 2002. Geologic map of the Death Valley ground-water model area, Nevada and California. US Geological Survey Miscellaneous Field Studies Map MF-2381-A.

Wright, L.A., Troxel, B.W., 1984. Geology of the North 1/2 Confidence Hills 15′ Quadrangle, Inyo County, California. Map Sheet 34, California Division of Mines and Geology. Scale 1:62,500.

Yaalon, D.H., Ganor, E., 1973. The influence of dust on soils during the Quaternary. Soil Science 116, 146–155.